

Precision polarization measurements of the $6s^2S_{1/2} \rightarrow 6p^2P_j$ Rayleigh scattering spectrum in atomic Cs

A. Markhotok, S. B. Bayram,^{a)} A. Sieradzan,^{b)} and M. D. Havey^{c)}
Department of Physics, Old Dominion University, Norfolk, Virginia 23529

(Received 17 December 2001; accepted for publication 7 May 2002)

A precision polarimeter has been developed to measure the linear polarization degree of Rayleigh scattered light. Application is made to measurement of the linear depolarization spectrum of atomic Cs in the vicinity of the $6s^2S_{1/2} \rightarrow 6p^2P_j$ resonance transition. For measurements in an $\sim 220 \text{ cm}^{-1}$ range around the $6s^2S_{1/2} \rightarrow 6p^2P_{3/2}$ resonance transition, the ratio of line strengths for the two resonance transitions has been found to be 2.003(52), in excellent agreement with other methods.

© 2002 American Institute of Physics. [DOI: 10.1063/1.1490151]

I. INTRODUCTION

One of the fundamental low energy interactions between electromagnetic radiation and atoms is nonresonant Rayleigh, or quasielastic light scattering.^{1,2} A century ago, the original article³ on this subject appeared, but the much later comprehensive work of Placzek⁴ presented the essential cross sections for both nonresonant Rayleigh and Raman scattering. Since that time there have been extensive studies of Rayleigh scattering of light by gases,² ranging from practical studies in which the intensity of Rayleigh scattered light serves as a density probe of the scattering gas to fascinating new phenomena associated with coherent scattering of light from a Bose–Einstein condensate⁵ of atomic Na. In addition, both calculations⁶ and measurements of Rayleigh scattering near nondegenerate levels have shown a strong polarization and frequency dependence to the scattered light intensity. In general, the polarization dependence occurs whenever there is light scattering from two or more levels of different angular momentum. Such phenomena have, for example, been observed for scattering in the spectral vicinity of $ns^2S_{1/2} \rightarrow np^2P_j$ fine structure multiplet transitions in atomic Na (Ref. 7) and in singly ionized Ba.⁸ Similar effects associated with the $3s^2S_{1/2} \rightarrow 3p^2P_{3/2}$ hyperfine multiplet in atomic Na have also been studied by Walkup *et al.*⁹ In the case of the $3s^2S_{1/2} \rightarrow 3p^2P_{3/2}$ measurements in Na,⁷ a discrepancy was noted between the experimental results and the theoretical expressions used to model them; a main focus of the present work is then to find whether a similar effect occurs for the depolarization spectrum of the Rayleigh scattered light associated with the atomic Cs resonance transitions.

Furthermore, although it is not the main emphasis of this article, it has been shown,¹⁰ that analysis of measurements of the polarization and frequency dependence of Rayleigh scattering can yield relative transition matrix elements. In some cases, particularly where there is a precisely known oscillator strength, it is then possible to put on an absolute scale the relative matrix elements for a series of multiplet transitions

(viz. $ns \rightarrow n'p$) in terms of this single fiducial value. Such an approach is more suited to Rayleigh scattering near transitions other than the resonance transition, for which contributions from other multiplet transitions are nearly negligible.

In this article we describe in detail the experimental technique we use to make precision polarization measurements of light Rayleigh scattered from an atomic gas. We also present measurements of the frequency-dependent polarization of Rayleigh scattering associated with the $6s^2S_{1/2} \rightarrow 6p^2P_j$ resonance transitions in atomic Cs. In this case, the light scattering is dominated by the two resonance transitions ($j=1/2,3/2$), and shows strong spectral and polarization-dependent interference associated with the coherent scattering off the two transitions. Furthermore, analysis of the measurements allows extraction of the ratio of line strengths for the two transitions. As this ratio is very well determined by other methods, it can serve as a figure of merit for the quality of the polarization measurements. In the remainder of this article, we present details of the experimental technique, followed by the experimental results and analysis. The results are then discussed in the context of other recent research in this area.

II. EXPERIMENT

The basic experimental scheme is illustrated in Fig. 1, which shows the lowest few energy levels¹¹ of atomic Cs. With reference to the figure, the energy, averaged over the hyperfine structure, of the $6s^2S_{1/2} \rightarrow 6p^2P_{3/2}$ transition is $\omega_{3/2} = 11\,732.35 \text{ cm}^{-1}$, while that of the $6s^2S_{1/2} \rightarrow 6p^2P_{1/2}$ transition is $\omega_{1/2} = 11\,178.24 \text{ cm}^{-1}$.¹² Note that more precise values^{13,14} are available for these transition energies, but the added precision has no effect on the present measurements. In terms of the frequency ω of the incident light, we define detuning from the $6s^2S_{1/2} \rightarrow 6p^2P_{3/2}$ transition as $\Delta = \omega - \omega_{3/2}$. In the present experiment, Δ is in the approximate range $\pm 110 \text{ cm}^{-1}$.

A block diagram of the experimental apparatus is shown in Fig. 2. In the figure, the laser is an Ar⁺ pumped titanium:sapphire ring laser. The laser is passively stabilized and provides an average power in the spectral range of the experiment of about 100–200 mW. The laser bandwidth is about 60 MHz, which includes characteristic drift and fluctuations

^{a)}Present address: Department of Physics, University of Michigan, Ann Arbor, MI 48109.

^{b)}Permanent address: Department of Physics, Central Michigan University, Mt. Pleasant, MI 48859.

^{c)}Electronic mail: mhavey@odu.edu

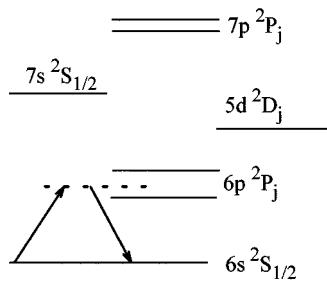


FIG. 1. Diagram of the lowest few energy levels in atomic Cs, illustrating the experimental scheme.

over the course of a typically 1-h experimental run. About 5% of the laser power is directed to a Burleigh WA-1500 wavemeter, which has a precision of about $\pm 10^{-3} \text{ cm}^{-1}$; the absolute calibration of the instrument was confirmed to $\sim 100 \text{ MHz}$ by measurement of the spectral location of the hyperfine components of the $6s^2S_{1/2} \rightarrow 6p^2P_{3/2}$ transition. The linear polarization of the laser output beam was purified with a Glan-Thompson prism, which has an extinction ratio of better than 10^{-5} . A Meadowlark liquid crystal variable retarder (LCR) was used to control the linear polarization direction of the laser beam to be in its natural state defined by the Glan-Thompson polarizer, or to rotate the linear polarization direction by $\pi/2$. A second Polarcor™ infrared polarizer used as an analyzer confirmed the purity of the resulting linear polarization to $\sim 10^{-4}$, and the angle between the two polarization states to $\leq 10^{-2}$ rad. The Polarcor™ infrared polarizer was employed in the detection arm to select a linear polarization direction of the scattered light to be normal to the plane formed by the wave vectors of the incident and scattered light.

The laser beam was weakly focused into a heated oven-cell arrangement that allowed control of the Cs cell temperature to $\pm 0.1 \text{ K}$ over the temperature range from 390 to 440 K used in the experiment. Typical operating temperature for data runs was in the range 390–400 K, corresponding to a Cs density $\sim 10^{13} \text{ cm}^{-3}$. The cylindrical Pyrex cell had two polished windows to minimize instrumental scattering, which at the largest detunings was less than 1% of the Rayleigh scattering signal. In addition, in order to accurately assess background light scattering, it was necessary to be able to quench the Cs density, and yet leave the cell oven and alignment

fixed. To do this, an $\sim 1 \text{ cm}$ long sidearm of radius about 3 mm extended from the cell and through a small hole in the oven. Directing a steady stream of compressed air to the tip of this sidearm reduced the Cs density by more than 10^3 in a few seconds, allowing the residual scattered laser radiation for each linear polarization state to be evaluated, also to about 1%, limited by counting statistics.

The scattered light was collected by a 35 mm field lens mounted in a precision translation stage. This allowed for sharp imaging of the interaction volume of the cell onto the slits of a 0.3 m spectrometer, which served as a spatial and spectral filter for the Rayleigh scattered light. As discussed in a later section, spectral filtering is important for detecting, and then removing unwanted signals due to atomic line fluorescence and molecular emission. For smaller detuning values, the spectrometer slits were typically adjusted to $40 \mu\text{m}$, well matched to the diameter of the laser beam in the interaction region. Increasing the slit width to $100 \mu\text{m}$ increased the signals considerably, but had no measurable effect on the measured polarization. The larger slit widths were used for detunings $\Delta > 100 \text{ cm}^{-1}$. The lens was stopped down to $f/16$, in order to make negligible depolarization due to the angular divergence of the scattered light. A linear polarization analyzer was mounted in front of the slits, and adjusted so that its transmission axis was collinear with that of the incident laser light; this adjustment was made with an accuracy of about $\leq 10^{-2}$ rad. The analyzing power of the polarimeter, including the LCR, the analyzing polarizer, and the combined effect of the angular divergence of the laser beams and the scattering signal is about 0.9995.

The scattered radiation was detected by a thermoelectrically cooled GaAs photomultiplier tube, which had a dark counting rate of a few Hz. The photon counting signals were processed with a fast preamplifier, and accumulated by a 100 MHz photon counter-discriminator system. Under the conditions of the experiment, the maximum counting rate was less than 10^4 s^{-1} , making dead time corrections negligible. Scanning of the spectrometer, wavemeter output, polarization switching, and acquisition and storage of signals were managed by a LabVIEW based computer-controlled data acquisition system.¹⁵ Automation of the instrumentation is essential to obtaining high quality measurements of the scattered light polarization. Of particular interest is the automation of the liquid crystal retarder, for which a special LabVIEW driver had to be written. Essentially, the software sends two 8 bit words to the LCR controller via the controlling-computer parallel port. These are sequentially latched and form the resulting 15 bit precision required to maintain the LCR retardance at the desired level. The commercially available LCR is temperature stabilized to $\pm 0.1 \text{ K}$, and the retardance across the $\sim 2.5 \text{ cm}$ available aperture is constant to about 1%. However, for the present application, in which the retarder is used as a $\lambda/2$ retarder for a laser beam having a cross-sectional area of a few millimeters, the analyzing power of the device can be as high as 0.9999.

During a typical experimental run, the Ti:sapphire laser output was adjusted to a selected detuning Δ , and the signals optimized. The spectrometer was then scanned discretely over a wavelength range sufficient to obtain the scattered line

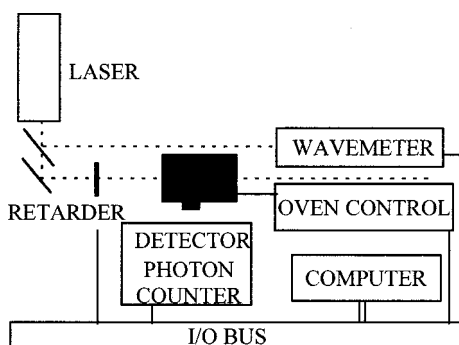


FIG. 2. Schematic diagram of the experimental apparatus.

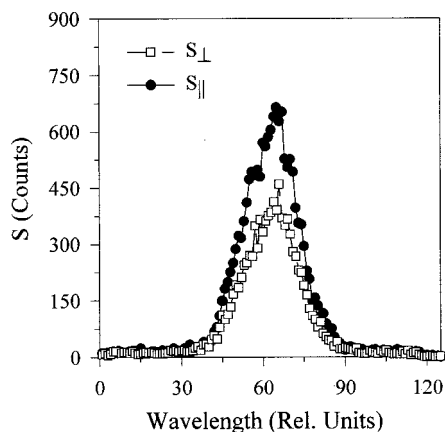


FIG. 3. Representative spectrometer scan over the Rayleigh scattering line for a detuning of -145.67 cm^{-1} , showing the polarization dependence of the signals.

and the baseline for the scattering signals. For each discrete setting of the spectrometer, the linear polarization direction of the laser beam was adjusted to be collinear and then perpendicular to the transmission axis of the analyzer in the detection arm. Defining the background corrected signal for collinear polarization as S_{\parallel} and for perpendicular polarization as S_{\perp} a linear polarization degree may be formed as

$$P_L = \frac{S_{\parallel} - S_{\perp}}{S_{\parallel} + S_{\perp}}. \quad (1)$$

Signals were accumulated for 1 s for each polarization state. Each scan of this type was divided into typically 400 steps, with the first 200 steps dedicated to the procedure above. For the second half of the scan, the direction of the spectrometer scan was reversed and the oven sidearm, described earlier, was cooled with a stream of cool air, effectively reducing the Cs density to negligible levels. With the polarization switching protocol the same, this reversed scan allowed the background of instrumentally scattered light to be reliably assessed. A typical scan of this type, which was taken at a detuning $\Delta = -145.670(2) \text{ cm}^{-1}$ and a temperature $T = 470 \text{ K}$, is shown in Fig. 3.

This type of scan is useful for evaluating the effects of background scattered light, for detecting possible signals due to Cs_2 molecular emission and for eliminating blending of the Rayleigh scattering line with collision-induced atomic emission on the $\text{Cs } 6s^2S_{1/2} \rightarrow 6p^2P_{3/2}$ transition. However, it is not optimum for obtaining good counting statistics for either the Rayleigh scattering signal or for measurement of instrumental background scattering. Instead, for final data runs the spectrometer was set at the peak of the Rayleigh scattering signal, and data accumulated for ~ 30 min, again with the first half reserved for signal acquisition and the second for background assessment. The protocol for polarization switching is the same in this case as in the previous one. Because of excellent alignment and laser power stability, reproducible polarization measurements at a $\pm 0.4\%$ level could be made, this being limited by counting statistics.

We conclude our discussion of the experimental instrumentation with some comments regarding some advantages

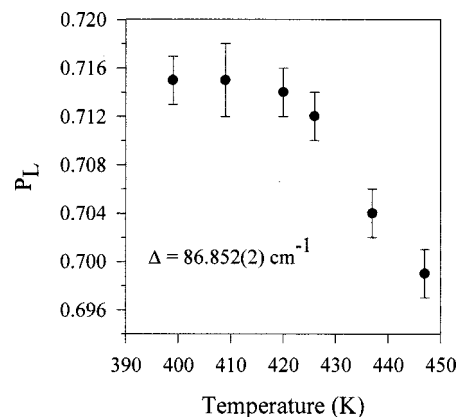


FIG. 4. Temperature dependence of the polarization of Rayleigh scattered light at a detuning of 86.85 cm^{-1} .

that our experimental approach has over other approaches. In general, we have taken advantage of the ability to electronically control and manipulate the instruments associated with the experiment. This has been achieved by taking care of thermal and mechanical stability of the apparatus, and to accumulate multichannel data sets that measure those quantities, such as laser power and frequency, that drift over a long data acquisition period. The experimental stability was such that, with computerized control of the experiment, runs longer than 5 h could routinely be achieved without intervention. This quality enables systematic effects to be reliably detected, on the one hand, and allows accumulation of sufficient signal to achieve the precision polarimetry reported in this article. This was a critical feature of the experiment, especially for the larger detunings as shown in Fig. 4.

Beyond this, precision and reliable digital control of the state of the laser polarization is a key element of the experiment. As the laser beam is very well collimated and is of small cross-sectional area, the analyzing power of the liquid crystal retarder could be optimized. This is to be compared to polarization analysis of the scattered light, where the significantly larger solid angle of detection degrades the peak achievable analyzing power. In other measurement approaches, a mechanically rotatable polarizer is frequently used,⁷ and phase sensitive detection employed to extract the polarization degree. As well as placing demands on long phase and alignment stability of the rotating devices, the sensitivity of the measurements is ultimately not as large. Then systematic effects that are difficult to assess, such as the temperature dependence illustrated in Fig. 3, may be virtually eliminated from the data.

III. RESULTS AND ANALYSIS

Polarization measurements were made over a Δ range $\sim 220 \text{ cm}^{-1}$ around the $6s^2S_{1/2} \rightarrow 6p^2P_{3/2}$ transition at $11\,732.35 \text{ cm}^{-1}$. The measurements were free of detectable systematic variations associated with laser power or with the signal counting rate. However, systematic reduction of the polarization was observed as a function of increasing cell temperature, which we attribute to background due to increasing Cs density. This background shows up in two ways. First, at higher cell temperature, there is, in addition to a

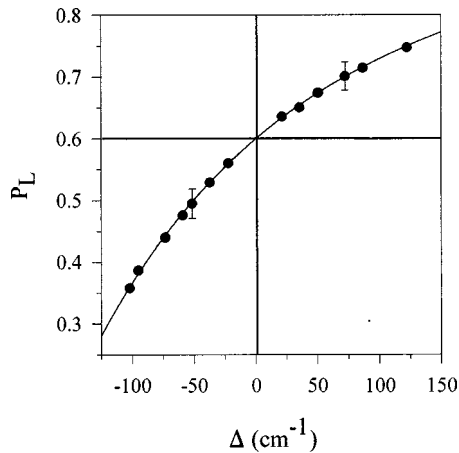


FIG. 5. Linear polarization spectrum of atomic Cs near-resonant Rayleigh scattering. The solid curve represents a least-squares fit to the data, with the minimum $\chi^2=2.567$.

strong Rayleigh scattering signal, intense unpolarized emission at the $6s^2S_{1/2} \rightarrow 6p^2P_{3/2}$ resonance transition, and weaker emission at the $6s^2S_{1/2} \rightarrow 6p^2P_{1/2}$ transition. Such emission has been observed previously in Rayleigh scattering experiments on the $3s^2S_{1/2} \rightarrow 3p^2P_j$ transitions in atomic Na,⁷ and attributed to collisional redistribution of the laser radiation to the resonance line via Na+Na binary collisions. In this experiment, this component increases with Cs density much faster than the Rayleigh scattering signal, suggesting that it is also due to binary alkali-alkali collisions. The conditions of the experiment were such that the resonance radiation is strongly self-absorbed, so no quantitative measurements were made of the relative cross sections for the two processes. Spectral and spatial filtering by the spectrometer greatly suppresses the effect of this emission on the Rayleigh scattering polarization. Second, for large spectral detunings, when the effects of collision-induced emission are negligible, a weak temperature dependence of the measured polarization of the Rayleigh scattered light was observed. This is illustrated in Fig. 4, which shows the linear polarization degree at $\Delta=86.852(2) \text{ cm}^{-1}$ as a function of temperature. It is seen that for temperatures above about 410 K there is a measurable decrease in the polarization with temperature. Spectrometer scans over the Rayleigh line revealed that for higher temperature there is a weak and nearly unpolarized background signal in the wings of the line. This signal is also likely due to Cs_2 molecular emission. For the purposes of this study, we indicate that temperature dependence was tested for all detunings used in this experiment, and final polarization measurements were made in temperature ranges where no variations with temperature were found.

The measured depolarization spectrum as a function of Δ is shown in Fig. 5. In this figure, the points are the average measured values for each detuning, while the solid curve represents a fit to the data as described in the following paragraph. Error bars on the points are negligible on the scale of the graph. The bars shown represent the statistical error on that polarization value magnified 10 times. Typical uncertainty in the detuning values is less than $\pm 0.01 \text{ cm}^{-1}$, this being due to drift of the laser frequency during a run. The

variation of P_L with Δ is primarily due to interference between the amplitudes for scattering on the $6s^2S_{1/2} \rightarrow 6p^2P_{1/2}$ and $6s^2S_{1/2} \rightarrow 6p^2P_{3/2}$ transitions. Expressions for the polarization-dependent scattering intensities may be readily derived, as was done originally in terms of oscillator strengths by Penney.⁶ They are given by

$$I_{\parallel} = I_o \left[\frac{2RM_{3/2}}{\Delta} + \frac{M_{1/2}}{\Delta + \Delta_f} + \frac{2RM_{3/2}}{\Delta - 2\omega} + \frac{M_{1/2}}{\Delta + \Delta_f - 2\omega} - p \right]^2, \quad (2)$$

$$I_{\perp} = I_o \left[\frac{RM_{3/2}}{\Delta} - \frac{M_{1/2}}{\Delta + \Delta_f} - \frac{RM_{3/2}}{\Delta - 2\omega} + \frac{M_{1/2}}{\Delta + \Delta_f - 2\omega} - q \right]^2. \quad (3)$$

In these expressions, all angular momentum coupling factors have been explicitly evaluated¹⁶ leaving normalized and squared transition matrix elements described by $M_{3/2}$ and $M_{1/2}$. Because of explicit evaluation of Racah coefficients in this expression, these squared radial matrix elements are nearly equal.¹⁷⁻²⁰ The quantities p and q represent the contributions to the scattering amplitudes from more energetic np multiplets. They are weakly frequency dependent and may be readily estimated from existing experimental,¹¹ or theoretical²¹ data to have the approximate values $p \sim -6.2 \times 10^{-5}$ and $q \sim 7.1 \times 10^{-6}$. They have a negligible effect on the polarization within the range and precision of the present experiment. This being the case, the factor $M_{1/2}$ may be removed from the above expressions, and the polarization parametrized by the line strength ratio $S = 2R \times M_{3/2}/M_{1/2}$.²² The quantity R is a parameter used to fit the data. In the present case, the factor $2M_{3/2}/M_{1/2}$ is extremely well known,²⁰ and has the value 1.9809(9). Thus adjustment of the parameter R to fit the experimental data allows comparison with this fiducial, with perfect agreement being obtained when $R = 1$.

In the expressions above, the effects of hyperfine structure on the intensities have been neglected. Although such effects are very pronounced⁹ for small detunings, they are negligible in the present case. In order to observe hyperfine-dependent variations in the light polarization, the hyperfine structure must be partially distinguished in both the lower and upper levels involved in the scattering. But for even the smallest detunings of the present study, the width of the excited state hyperfine manifold is less than 10^{-3} of the detuning Δ . Under these circumstances the hyperfine-dependent denominators may be neglected and the F -dependent angular momentum factors reduce to the M_j above. Here F is the combined total of atomic and nuclear angular momentum.

We have made a least-squares fit of the 127 individual polarization data points to the equations above, using R as an adjustable parameter to minimize the reduced χ^2 . In the fit, contributions from the $n=7-8 \text{ np}$ multiplets were included, but held at the numerical values indicated above. A minimum was found at $\chi^2=2.567$ for $R=1.011(26)$, where the quoted uncertainty in the last digit represents one standard deviation. This implies a line-strength ratio of 2.003(52), which is to be compared to other values in Table I. The result of the fit is

TABLE I. Summary of experimental and theoretical line strength ratios for the Cs resonance transitions.

Lifetime ^a	1.984(8)
Lifetime ^b	1.977(8)
Absorption ^c	1.9809(9)
MBPT ^d	1.9817
This work	2.003(52)

^aReference 18.

^bReference 19.

^cReference 20.

^dReference 24.

also displayed in Fig. 6, where the residuals of the fit are shown, along with the error bars associated with each polarization value. The polarization residuals are represented as $P_L(\text{calculated}) - P_L(\text{measured})$. As seen Fig. 6, the mean residual is consistent with zero, and about 2/3 of the data points are located within the indicated $\pm 1\sigma$ error bounds, representing nearly an ideal fit with statistical errors only. For comparative purposes, an alternative analysis was done, where the 13 average polarization measurements, and associated standard deviations, were again fit to the theoretical expressions above. For this fit, a minimum was found at $\chi^2 = 0.397$ for $R = 1.007(35)$, where the quoted uncertainty in the last digit again represents one standard deviation. The values for R are consistent for the two cases, with the reduction in the χ^2 minimum value not surprising for the smoothed average polarization data set.

The overall shape of the polarization curve²³ in Fig. 5 is similar to that measured previously⁷ in the vicinity of the Na resonance lines. In fact, as indicated by Tam and Au,⁷ if only the two largest terms are kept in the expressions for the scattered intensity, then the quantity $1/(1 - P_L)$ is of Lorentzian form with a width $\Delta_f/3$, so long as $R \sim 1$. However, the discrepancy between the measured and calculated polarization degree found in Na was not found in the present work on Cs. It is possible that the discrepancy found in Na is due to a weak undetected molecular emission, similar to that observed in the present experiment.

There have been several recent precision measurements of the lifetimes of the Cs resonance transitions,¹⁷⁻¹⁹ includ-

ing a very precise determination of the line-strength ratio by Rafac and Tanner.²⁰ The lifetime measurements of Tanner *et al.*¹⁹ are done using meticulous measurements of decay of excited Cs atoms along their flight path in an atomic beam. Those of Young *et al.*¹⁹ employ femtosecond excitation of a Cs atomic beam, and time-correlated single-photon counting to extract the lifetimes of the $6s^2S_{1/2} \rightarrow 6p^2P_{1/2}$ and $6s^2S_{1/2} \rightarrow 6p^2P_{3/2}$ transitions. In order to facilitate comparison, the lifetime values and the measurements of the ratio R have been converted to the line-strength ratio for the two transitions. The line strength depends on the reduced matrix elements for the transition, but does not explicitly remove the recoupling coefficients as in Eq. (2). These experimental values are presented in Table I, along with the line-strength ratio determined by the direct absorption measurements of Rafac and Tanner. Also included for comparison is a line-strength ratio derived from recent relativistic many-body perturbation theory calculations.^{21,24} It is seen from these values that there is excellent agreement among the various experimental determinations of the line-strength ratio, in spite of the very different experimental approaches used to determine them. Because the spectral variations in the polarization spectrum that influence the determination of the line strength occur at large detunings for the Cs resonance lines, the technique used in the present study is not suitable for determining line-strength ratios in this case to the precision of the best lifetime and absorption measurements. However, for transitions to more highly excited multiplets, particularly the np ($n > 6$) multiplets in Cs, the important spectral regions are in an approximately $\pm 10 \text{ cm}^{-1}$ range around the atomic resonances. This suggests that the technique described in this paper may be effectively used to determine matrix element ratios for transitions involving more highly excited levels, including the $ns^2S_{1/2} \rightarrow n'p^2P_j$ principal transitions in the alkali atoms or alkaline earth ions.

IV. CONCLUSIONS

An instrument has been developed for making precision linear polarization measurements of light Rayleigh scattered from gaseous samples. Using this device, measurements of the polarization spectrum of Rayleigh scattered light in the vicinity of the atomic Cs resonance lines have been made. The spectrum displayed distinctive interference structure associated with the amplitude for scattering from the two fine-structure multiplet components. In addition, at higher Cs density strong but unpolarized redistribution of the incident radiation by Cs+Cs collisions to the atomic resonance lines was observed. This observation did not have a measurable effect on the low-density polarization spectrum used in further analysis of the polarization spectrum. Analysis allowed determination of the line-strength ratio for the resonance transitions. The ratio was found to be in excellent agreement with earlier measurements using quite different techniques, but was not so precise. However, the quality of the measurements is such that they may now be extended to other resonance transitions for which the line strength ratio is not well known, and for which other approaches are not so readily applied. In particular, the Rayleigh scattering technique is

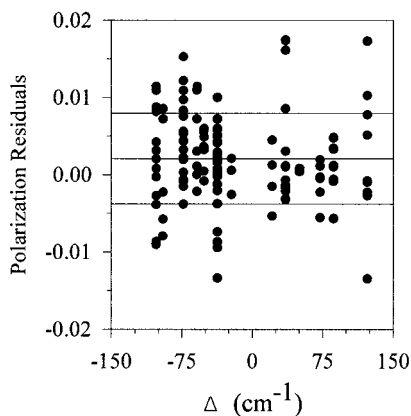


FIG. 6. Deviation $P_L(\text{fit}) - P_L(\text{measured})$ between the fit and the experimental data points.

now being extended to measurements on more highly excited–state transitions, including the $6s\ ^2S_{1/2} \rightarrow 7p\ ^2P_j$ transitions in Cs, for which neither the absolute or relative values are precisely known. These relative values can be put on an absolute scale by reference to the well-known strength of the Cs resonance transitions.¹⁰

¹C. Cohen-Tannoudji, J. Dupont-Roc, and G. Grynberg, *Atom-Photon Interactions: Basic Processes and Applications* (Wiley, New York, 1992).

²D. Marcuse, *Principles of Quantum Electronics* (Academic, New York, 1980).

³Lord Rayleigh, *Philos. Mag.* **47**, 375 (1899).

⁴G. Placzek, *Handbuch der Radiologie, VI* (Akademische, Leipzig, 1934), Vol. 2, p. 209.

⁵S. Inouye, A. P. Chikkatur, D. M. Stamper-Kurn, J. Stenger, D. E. Pritchard, and W. Ketterle, *Science* **285**, 571 (1999).

⁶C. M. Penney, *J. Opt. Soc. Am.* **59**, 34 (1969).

⁷A. C. Tam and C. K. Au, *Opt. Commun.* **19**, 265 (1976).

⁸G. Chen and T.-J. A. Nee, *J. Opt. Soc. Am. B* **4**, 1303 (1987).

⁹R. Walkup, A. L. Migdall, and D. E. Pritchard, *Phys. Rev. A* **25**, 3114 (1982).

¹⁰M. D. Havey, *Phys. Lett. A* **240**, 219 (1998).

¹¹A. A. Radzig and B. M. Smirnov, *Reference Data on Atoms, Molecules and Ions* (Springer, Berlin, 1985).

¹²C. E. Moore, *Atomic Energy Levels* (U.S. Government Printing Office, Washington, DC, 1971).

¹³Th. Udem, J. Reichert, R. Holswarth, and T. W. Hansch, *Phys. Rev. Lett.* **82**, 3568 (1999).

¹⁴G. Avila, P. Gain, E. de Clercq, and P. Cerez, *Metrologia* **22**, 111 (1968).

¹⁵Development by SciNet VI (1999).

¹⁶M. E. Rose, *Elementary Theory of Angular Momentum* (Wiley, New York, 1957).

¹⁷C. E. Tanner, A. E. Livingston, R. J. Rafac, F. G. Serpa, K. W. Kukla, H. G. Berry, L. Young, and C. A. Kurtz, *Phys. Rev. Lett.* **69**, 2765 (1992).

¹⁸R. J. Rafac, C. E. Tanner, A. E. Livingston, K. W. Kukla, H. G. Berry, and C. A. Kurtz, *Phys. Rev. A* **50**, R1976 (1994).

¹⁹L. Young, W. T. Hill III, S. J. Sibener, S. D. Price, C. E. Tanner, C. E. Wieman, and S. R. Leone, *Phys. Rev. A* **50**, 2174 (1994).

²⁰R. J. Rafac and C. E. Tanner, *Phys. Rev. A* **58**, 1087 (1998).

²¹S. A. Blundell, W. R. Johnson, and J. Sapirstein, *Phys. Rev. A* **43**, 3407 (1991).

²²I. I. Sobelman, *Atomic Spectra and Radiative Transitions* (Springer, Berlin, 1996).

²³Spectrum of the scattered light is often called a depolarization spectrum, reflecting the departure of the linear polarization from the value of 100% expected for a classical oscillator. Here we refer to the spectrum in terms of the measured linear polarization degree defined in Eq. (1).

²⁴S. A. Blundell, J. Sapirstein, and W. R. Johnson, *Phys. Rev. D* **45**, 1602 (1992).